

Identification of immunotherapeutic targets by genomic profiling of rectal NET metastases

Zeynep Koşaloğlu^{a,b}, Inka Zörnig^b, Niels Halama^b, Iris Kaiser^b, Ivo Buchhalter^c, Niels Grabe^b, Roland Eils^{c,d}, Matthias Schlesner^c, Andrea Califano^e, and Dirk Jäger^{a,b}

^aClinical Cooperation Unit “Applied Tumor Immunity”, National Center for Tumor Diseases (NCT) and German Cancer Research Center (DKFZ), Heidelberg, Germany; ^bDepartment of Medical Oncology, National Center for Tumor Diseases (NCT) and University Hospital Heidelberg, Heidelberg, Germany; ^cDivision of Theoretical Bioinformatics (B080), German Cancer Research Center (DKFZ), Heidelberg, Germany; ^dDepartment for Bioinformatics and Functional Genomics, Institute for Pharmacy and Molecular Biotechnology (IPMB) and BioQuant, Heidelberg University, Heidelberg, Germany; ^eDepartment of Biomedical Informatics, Department of Systems Biology, Center for Computational Biology and Bioinformatics, Herbert Irving Comprehensive Cancer Center, Columbia University, New York, NY, USA

ABSTRACT

Neuroendocrine tumors (NETs) of the gastrointestinal tract are a rare and heterogeneous group of neoplasms with unique tumor biology and clinical management issues. While surgery is the only curative treatment option in patients with early stage NETs, the optimal management strategy for patients with advanced metastatic NETs is unknown. Based on the tremendous success of immunotherapeutic approaches, we sought to investigate such approaches in a case of metastatic rectal NET. Here, we apply an integrative approach using various computational and experimental methods to explore several aspects of the tumor–host immune interactions for immunotherapeutic options. Sequencing of six different liver metastases revealed a quite homogenous set of mutations, and further analysis of these mutations for immunogenicity revealed few neo-epitopes with pre-existing T cell reactivity, which can be used in therapeutic vaccines. Staining for immunomodulatory proteins and cytokine profiling showed that the immune setting is surprisingly different, when compared to liver metastases of colorectal cancer for instance. Taken together, our results highlight the broad range and complexity of tumor–host immune interaction and underline the value of an integrative approach.

Abbreviations: HLA, human leukocyte antigen; indel, short insertion or deletion; NET, neuroendocrine tumor; RNA-Seq, RNA-sequencing; RPKM, reads per kilobase per million reads; SNV, single nucleotide variation; WGS, whole-genome-sequencing

Introduction

Neuroendocrine tumors (NETs) represent an extremely heterogeneous group of tumors. NETs develop from neuroendocrine cells at various primary organ sites and are grouped according to their origin: the foregut, the midgut, and hindgut.¹ The majority of NETs are found throughout the intestinal tract, most commonly in the pancreas. NETs of the colon and rectum are rare, comprising less than 1 percent of colon and rectal cancers, and rectal NETs constitute about 19 percent of all gastrointestinal NETs.^{2,3}

Despite the considerable advances made in recent decades, the genetic and molecular determinants of NET tumor biology remain poorly characterized.⁴ Pathological features found in many NETs are poor differentiation, distinctive expression of neuroendocrine markers, and the ability to secrete bioactive peptides.⁵ Around 20% of NETs occur in the context of genetic syndromes, for instance the multiple endocrine neoplasia type 2 (MEN-2) syndrome which is caused by germline gain of function mutations in the protooncogene RET. A wide range of

somatic genetic alterations have also been described for various NETs, hindgut NETs however remain poorly characterized.^{4,6,7} Generally, NET genomes harbor relatively few somatic mutations when compared with adenocarcinomatous tumors.⁶

NETs present a wide spectrum of malignancies from relatively indolent to highly aggressive variants. The prognosis for high-grade poorly differentiated neuroendocrine carcinomas however is generally poor, as most patients have metastatic disease at the time of diagnosis, whereas patients with low-grade NETs have a rather favorable prognosis.² The low incidence of neuroendocrine carcinomas coupled with their variable clinical manifestation was a major barrier to investigation, and advances in the treatment of NETs have been slow. Optimal treatment of NETs has been widely debated and remains to be controversial. Response to chemotherapy has been traditionally poor for low-grade NETs with an unfavorable benefit-to-risk ratio. When feasible, surgical removal of malignant tissue is the primary treatment option for NETs and offers the best prognosis.^{8,9}

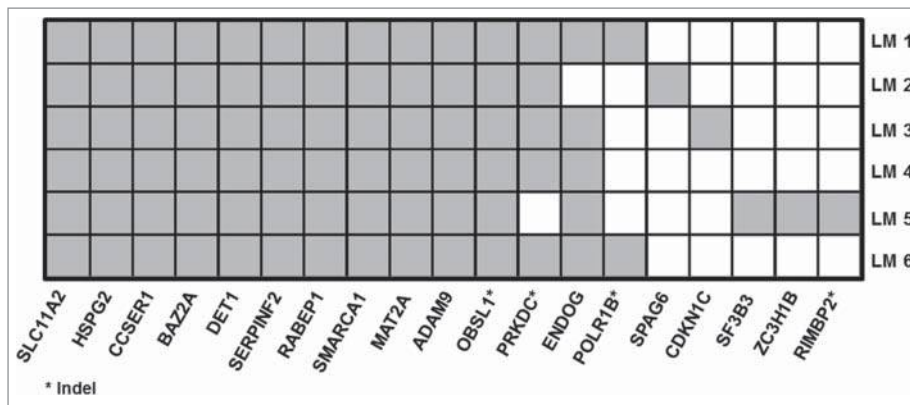


Figure 1. Mutational landscape of all analyzed liver metastases. Whole-Genome-Sequencing and Whole-Transcriptome-Sequencing was performed on six different liver metastases as well as on healthy liver tissue and whole-blood of the same patient. Single nucleotide variations (SNVs) as well as indels (short insertions or deletions) were detected in each of the sequences. A gray cell indicates a somatic mutation in the corresponding gene and metastasis, an asterisk indicates an indel.

Due to the highly heterogeneous nature of most NETs, a personalized treatment strategy might be an appropriate approach and it has been suggested, that genome-wide screening for mutations may reveal new data that can be used for a more appropriate treatment selection.⁴ Furthermore, immunotherapies such as vaccinations against neoantigens and checkpoint blockade therapies have shown dramatic success in a number of tumor entities (for a review see refs.¹⁰ and¹¹), and it has been suggested, that immunotherapy in NETs provides opportunities for future advances.^{1,6} However, it is largely unclear how the setup of the immunological microenvironment in metastatic NET is and especially how diverse these mutations and immunological setups can be between different metastatic lesions.

In this study, we characterized the genomic features of an individual metastatic NET of the rectum, by whole-genome and RNA-sequencing analysis (WGS and RNA-Seq) of six metastatic lesions (Table 1). It has been repeatedly shown, that individual, tumor-specific mutations found in the genome of cancer patients provide a superior source of immunogenic targets. Mutation-derived epitopes, so called neo-epitopes, are expressed in a highly tumor-specific manner, and are also expected to overcome central tolerance. We identified several neo-epitopes in the tumor samples, which are suitable candidates for peptide- or RNA-based vaccines. We furthermore characterized the immunological features of the tumor by assessing the density of lymphocyte infiltration into the metastatic site, as well as the expression of immunomodulatory proteins, as it is known, that these can be indicators for disease progression and immunotherapy outcome. We also measured existing immune responses against several predicted neo-epitopes from the peripheral blood of the same patient.

Here, we present a unique dataset covering different aspects of tumor immunology. Our data give a comprehensive insight into the immune setting of a metastatic NET of the rectum, and nicely demonstrates our integrative analysis workflow for the prediction of mutation-derived neo-epitopes and profiling of the immunological tumor microenvironment leading to the identification of suitable immunotherapeutic target molecules.

Results

Somatic mutations

A total of 55 non-synonymous somatic coding SNVs and seven indels were detected in the WGS data, of which 15 SNVs and four indels were also found to be expressed according to the RNA-Seq data (Supplementary Table). Expressed mutations in 11 genes were found in all of the six liver metastases, and additional two mutations were found in the majority of the liver metastases. One mutation was detected in two samples and the remaining five mutations were unique to one sample (Fig. 1 and Table 2).

Epitopes

For the prediction of neo-epitopes, we only considered expressed SNVs and indels that were present in the majority of

Table 1. Overview of analyzed samples.

Sample	Year of surgery	Information	Detected mutations
LM1	2010	NA	14
LM2	2012	piece of tumor from a 2 cm lesion from posterior segment 2, left lobe	13
LM3	2012	piece of tumor from a 2 cm lesion from the left lobe of the liver, segment 4	14
LM4	2012	piece of tumor from a 3 cm lesion from the right lobe of the liver, segment 4	13
LM5	2012	piece of tumor from a 1 cm lesion from the right lobe of the liver (i.e., close to the edge of the liver).	15
LM6	2012	piece of tumor from the 8 cm major lesion from the right lobe of the liver (i.e., close to the middle of the liver) note: this lesion was largely hemorrhagic	14

Table 2. Overview of detected expressed mutations.

Gene	Chr	Pos	Ref	Alt	classification	#of affected samples	Affected samples	Epitopes predicted
SLC11A2	12	51382161	T	C	Non-synonymous SNV	6	LM1;LM2;LM3;LM4;LM5;LM6	1
HSPG2	1	22150143	G	T	Non-synonymous SNV	6	LM1;LM2;LM3;LM4;LM5;LM6	1
CCSER1	4	92519846	A	G	Non-synonymous SNV	6	LM1;LM2;LM3;LM4;LM5;LM6	0
BAZ2A	12	57003963	C	G	Non-synonymous SNV	6	LM1;LM2;LM3;LM4;LM5;LM6	0
DET1	15	89074654	C	A	Non-synonymous SNV	6	LM1;LM2;LM3;LM4;LM5;LM6	0
SERPINF2	17	1655979	G	A	Non-synonymous SNV	6	LM1;LM2;LM3;LM4;LM5;LM6	4
RABEP1	17	5264636	G	T	Non-synonymous SNV	6	LM1;LM2;LM3;LM4;LM5;LM6	1
SMARCA1	X	128599617	C	G	Non-synonymous SNV	6	LM1;LM2;LM3;LM4;LM5;LM6	2
MAT2A	2	85770808	G	T	Non-synonymous SNV	6	LM1;LM2;LM3;LM4;LM5;LM6	3
ADAM9	8	38880677	G	A	Non-synonymous SNV	6	LM1;LM2;LM3;LM4;LM5;LM6	5
OBSL1	2	220416342	GC	G	frameshift deletion	6	LM1;LM2;LM3;LM4;LM5;LM6	9
PRKDC	8	48701554	G	GT	frameshift insertion	5	LM1;LM2;LM3;LM4;LM6	0
ENDOG	9	131581121	C	T	Non-synonymous SNV	5	LM1;LM3;LM4;LM5;LM6	5
POLR1B	2	113333084	A	AGATCG	frameshift insertion	2	LM1;LM6	NA
SPAG6	10	22705558	C	T	Non-synonymous SNV	1	LM2	NA
CDKN1C	11	2905268	G	A	Non-synonymous SNV	1	LM3	NA
SF3B3	16	70582330	C	T	Non-synonymous SNV	1	LM5	NA
ZC3H18	16	88690471	G	A	splicing	1	LM5	NA
RIMBP2	12	130926721	GC	G	frameshift deletion	1	LM5	NA

samples. Hence, 13 mutations were considered and peptides with a predicted binding affinity lower than 500 nM were considered as binders. As a result, 19 peptides from eight mutated genes were predicted to bind with high to intermediate affinity to one of the patient's HLA alleles (Table 3). Seven peptides were predicted to bind to HLA-A, 14 to HLA-C, and no peptides were predicted to bind to HLA-B.

Thirteen of the mutated peptides have better predicted binding affinities compared to the cognate wild-type peptide. Seven mutated/wild-type peptide pairs have comparable predicted binding affinities, and for one peptide, the wild-type peptide has a better affinity than the mutated counterpart. Two mutated peptides were predicted to bind by both HLA-C08 and HLA-C03.

Table 3. Overview of predicted neo-epitopes.

Gene:Mutation	Mutated			Wild-type			HLA	Gene expression fold change (log2)
	Peptide ID	MT epitope	MT affinity (nM)	Peptide ID	WT epitope	WT affinity (nM)		
ADAM9:M249I	ADAM9-mt1	DSIYIMLNIR	37.92	ADAM9-wt1	DSMYIMLNIR	33630.31	A33	2.21
	ADAM9-mt2	YLDSIYIM	16.3	ADAM9-wt2	YLDSEYIM	14.56	C08	
	ADAM9-mt3	YLDSIYIML	461.65	ADAM9-wt3	YLDSEYIML	13.56	C03	
		YLDSIYIML	12.61	YLDSIYIML	13.56	C08		
ENDOG:P53L	ADAM9-mt4	YLDSIYIMLNI	37.81	ADAM9-wt4	YLDSEYIMLNI	37.61	C08	-0.16
	ENDOG-mt1	AAAELPL	311.03	ENDOG-wt1	AAAELPP	25109.54	C03	
	ENDOG-mt2	AAAELPLV	479.1	ENDOG-wt2	AAAELPPV	663.31	C08	
	ENDOG-mt3	ELPLVPGGPR	377.91	ENDOG-wt3	ELPPVPGGPR	28319.21	A33	
	ENDOG-mt4	VAAAAELPL	179.12	ENDOG-wt4	VAAAAELPP	19563.17	C03	
HSPG2:N4323K MAT2AK367N	HSPG2-mt	LVSGRSPGPK	443.88	HSPG2-wt	LVSGRSPGN	36429.09	A03	-0.1
	MAT2A-mt1	DLDLNKPIYQR	261.59	MAT2A-wt1	DLDLKKPIYQR	39619.11	A33	
	MAT2A-mt2	DLNKPIYQR	18.67	MAT2A-wt2	DLKKPIYQR	44256.9	A33	
	MAT2A-mt3	LNKPIYQR	270.22	MAT2A-wt3	LKKPIYQR	47740.48	A33	
RABEP1: S410I SERPINF2:D204N	RAPEP1-mt	STDILGTSGSL	49.63	RAPEP1-wt	STDILGTSGSL	47.75	C08	0.59
	SERPINF2-mt1	LANLSWNTL	279.13	SERPINF2-wt1	LANLSWDTL	533.92	C03	
		LANLSWNTL	338.95	LANLSWDTL	533.92	C08		
	SERPINF2-mt2	LSWNTLHPPL	412.08	SERPINF2-wt2	LSWDTLHPPL	843.61	C03	
	SERPINF2-mt3	LSWNTLHPPLV	461.83	SERPINF2-wt3	LSWDTLHPPLV	366.71	C08	
SLC11A2:S541G SMARCA1:L958F	SLC11A2-mt	FLDCGHTVGI	29.72	SLC11A2-wt	FLDCGHTVSI	14.71	C08	1.42
	SMARCA1-mt1	RFICMLHK	264.16	SMARCA1-wt1	RFLICMLHK	40457.46	A03	
SMARCA1-mt2	YTEEEDRFFI	331.66	SMARCA1-wt2	YTEEEDRFLI	336.3	C08		
OBSL1:neoORF	OBSL1-neoORF1	MTFDLRTK	46.66				A03	2.3
	OBSL1-neoORF2	MTFDLRTK	205.07				A33	
		SSMTFDLR	158.39				A03	
		SSMTFDLR	439.71				A33	
	OBSL1-neoORF3	SSMTFDLRTK	188.66				A03	
	OBSL1-neoORF4	HSWSSMTFDLR	243.03				A03	
		HSWSSMTFDLR	38.12				A33	
	OBSL1-neoORF5	SMTFDLRTK	470.27				A03	
	OBSL1-neoORF6	DLRTKALTAAR	34.03				A33	
	OBSL1-neoORF7	LTAARPAR	80.00				A33	
OBSL1-neoORF8	RTKALTAAR	96.68				A33		
OBSL1-neoORF9	MTFDLRTKAL	454.22				C03		

A frameshift deletion in the gene *OBSL1* generates a novel peptide of 28 amino acids. In these peptides, nine 8–11mer peptides were predicted to bind with high to intermediate affinity to one of the patient's HLA alleles. Three peptides were predicted to bind both HLA-A03 and HLA-A33.

For the mutated genes harboring predicted epitopes, the RPKM values were calculated using RNA-Seq data from healthy liver tissue and tumor tissue to assess changes in gene expression. For six of these eight genes, namely *ADAM9*, *MAT2A*, *RABEP1*, *SLC11A2*, *SMARCA1*, and *OBSL1*, gene expression is increased in the tumor, with *ADAM9* and *OBSL1* being highly over-expressed in the tumor with a fold change of over 2.

ELISPOT

To assess whether there are T cells in the patient's peripheral blood that are reactive against the predicted neo-epitopes, we conducted IFN γ ELISpot assays. As negative control, DCs were loaded with human IgG and antigen-specific T cell reactivity was assumed if spot numbers in triplicate test wells significantly exceeded those of control wells. An overview image of the IFN γ ELISpot plate with patient-derived cells and quantitative data of this plate presented in Fig. 2.

The peptides *MAT2A*-mt3, *MAT2A*-wt3, *RABEP1*-mt, *RABEP1*-wt, *SERPINF2*-wt3, and *OBSL1*-neoORF3 showed higher spot numbers when compared to the spot counts of control wells, indicating that there are reactive T cells in the peripheral blood against the tested peptides.

Immunohistochemistry and cytokine analysis

The samples LM3, LM4, and LM5 were immunohistochemically stained to analyze the presence of lymphocytes and the expression of immunomodulatory proteins. In order to assess, whether epitope presentation is altered, we analyzed HLA class I expression and interestingly, a uniform HLA class I expression among all analyzed samples could be detected in our immunohistochemical stainings. T cell and B cell numbers at the metastatic sites are generally very low, and even absent in many parts of the analyzed metastases. Not surprisingly, cell numbers for NK cells are also generally low. Concordant with the low infiltration of effector T cells, PD-1, and PD-L1 are also only found in low levels in the analyzed tissues (Fig. 3).

The metastatic tissue LM6 was used for the analysis of 50 cytokines and chemokines. Protein concentrations of the analyzed cytokines were found to be quite low and the measured cytokines do not reflect a Th1 or Th2 cytokine profile. Only a small subset of cytokines, namely MIF, VCAM-1, and ICAM-1, are expressed in a significant concentration, compared to normal adjacent liver (Fig. 4).

Discussion

NETs of the gastrointestinal tract are a rare and heterogeneous group of neoplasms with a unique tumor biology and clinical management issues. While surgery is the only curative treatment option in patients with early stage NETs, the optimal management strategy for patients with advanced metastatic

NETs is unknown. Based on the tremendous success of immunotherapeutic approaches, we sought to investigate such approaches in a case of metastatic rectal NET.

As known from studies on other NET types, the total number of somatic mutations is low compared to other tumor entities. In our case, between 13 and 15 expressed mutations were detected in each sample and 19 distinct mutations were found in all samples together.

Comparing the mutated genes from all liver metastases, it is striking that the overlap between them is quite large. A set of 13 mutations can be found nearly in all analyzed liver metastasis samples, regardless of their spatial and temporal differences. In cancer, it is usually observed that the tumors acquire more mutations with disease progression, and emerging evidence suggests that genetic abnormalities vary substantially between metastases or even within a single tumor mass, indicating intra-tumor heterogeneity.^{12–14} Determining the impact of such clonal structures still requires future studies. Intra-tumoral heterogeneity has important consequences for personalized-medicine approaches. Several clinical observations of different tumor types have shown variability in response to therapy that can occur between metastases or within a single-tumor mass.^{15–18} This variability may be explained by the emergence of genomically distinct clones of malignant cells.

We could not observe any major clonal variation in the metastases of this rectal NET patient, as there is a striking overlap of mutated genes. This may be due to the indolent nature of neuroendocrine tumors compared to their adenocarcinomatous counterparts. Thirteen mutations are shared among nearly all analyzed metastases. This fact alone indicates a central role of these genes in disease progression. Exploring the molecular functions of these mutated genes revealed some insights which may indicate a role in tumorigenesis.

HSPG2 encodes the protein perlecan which is a large multi-domain proteoglycan that binds and cross-links cell surface molecules. Due to its many interactions, perlecan plays essential roles in multiple biological activities, such as vascularization and angiogenesis, and might hence contribute to disease progression in this patient.¹⁹ It was suggested, that the protein encoded by *SMARCA1*, also called *SNF2L*, may play a role in DNA damage, growth inhibition, and apoptosis of cancer cells.^{20,21} Thus, we can assume that a non-synonymous mutation in *SMARCA1* could contribute positively to tumorigenesis. Another interesting mutated gene is *SERPINF2*. This gene encodes a member of the serpin family of serine proteases and the proper function of this gene has a major role in regulating the blood clotting pathway. Mutations of *SERPINF2* are characterized by severe hemorrhage, which was also observed in metastasis LM6 in our case.

Mutated antigens greatly contribute to the immunogenicity of human tumors. A single nucleotide variation can potentially lead to the production of various new antigenic peptides (neoantigens) that can be recognized by autologous T cells. Additionally, so called neoORF antigens can be generated by frameshifting insertions or deletions, which are supposed to be completely novel and were also shown to be recognized by autologous T cells.^{22–24}

These neoantigens are highly attractive as immunotherapeutic targets as they are expected to overcome central tolerance,

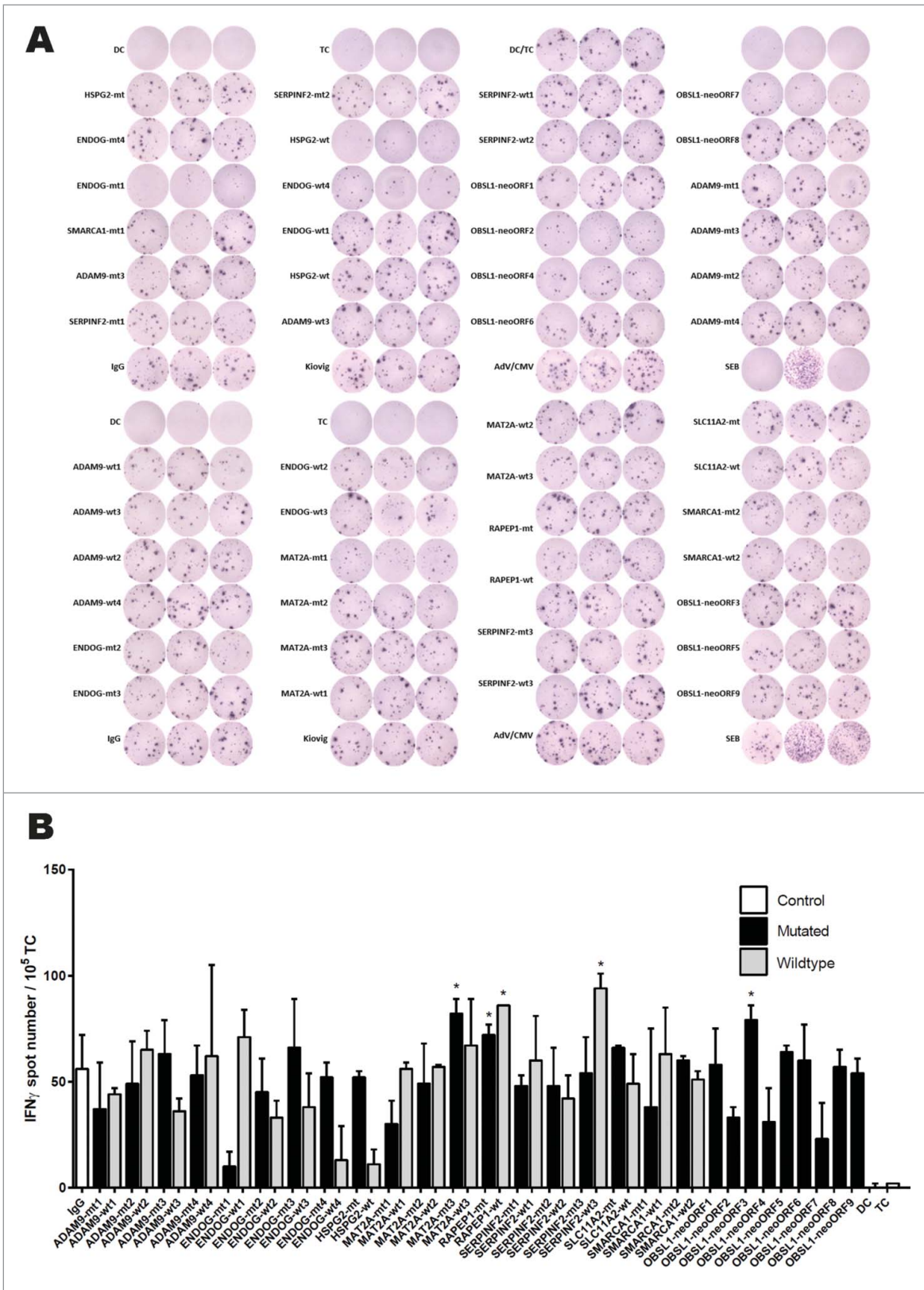


Figure 2. Overview of IFN γ ELISpot data for all tested neo-epitopes and controls with patient-derived cells. Peripheral blood dendritic cells (DCs) were pulsed with mutated and corresponding wild-type peptides as well as negative control antigen (human IgG), and incubated with autologous T cells. ELISpot assays were performed in triplicates. (A) Triplicate wells from IFN γ ELISpot analysis of all tested peptides. (B) Summary of ELISpot data showing mean spot number + SD for each tested peptide. An asterisk indicates significantly higher spot numbers in test wells compared with spot numbers of negative control antigen.

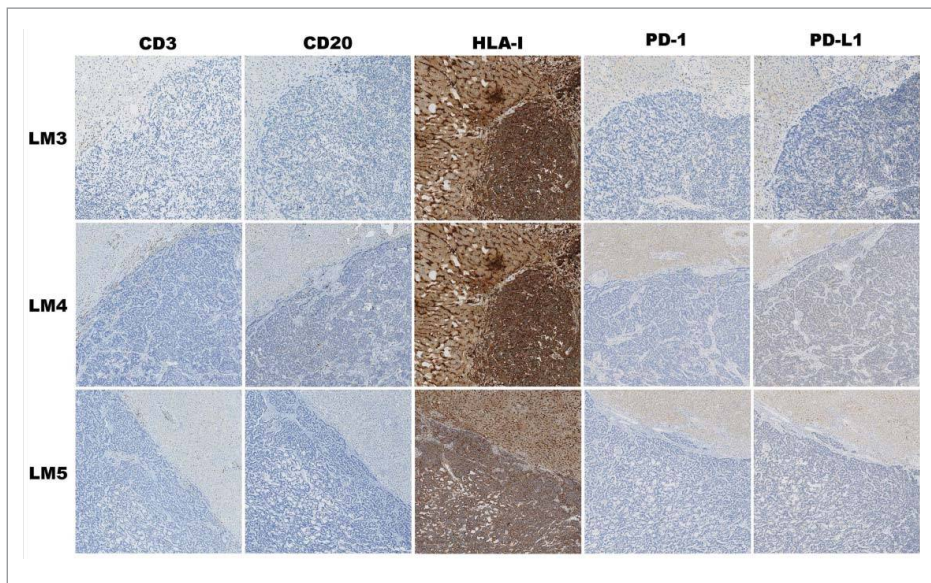


Figure 3. Immunohistochemistry. The samples LM3, LM4, and LM5 were immunohistochemically stained to analyze the presence of lymphocytes (CD3 and CD20), and the expression of HLA and the immunomodulatory proteins PD-1 and PD-L1. Images of LM3 show 1 mm² with a magnification of 9x, images of LM4 and LM5 show 4 mm² with a magnification of 4.5x.

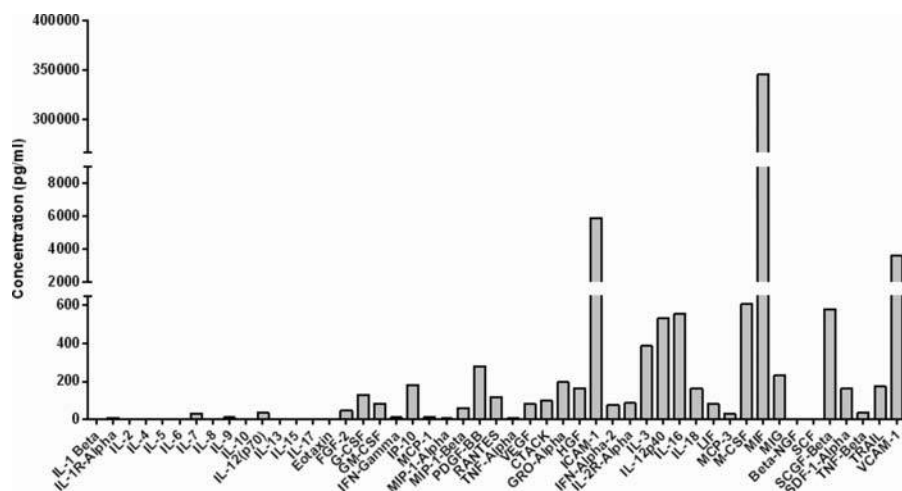
and their expression is tumor-specific.^{25,26} On the basis of animal model data, proof-of-principle for the feasibility to identify T cell reactivity against patient-specific neoantigens through the exploitation of genome data was obtained.^{27,28} It was also shown in numerous studies in mouse models that vaccination with predicted neoantigens results in increased tumor control.^{27,29-31} In subsequent studies in humans it has then been demonstrated that tumor sequencing data can also be exploited in a clinical setting, and that neoantigens serve as tumor-rejection antigens.^{30,32-35}

As no standard treatment for metastatic NETs was established yet, and because NETs are known to be highly heterogeneous and unique regarding the genomic landscape, we suggest, that a personalized treatment strategy, targeting patient-specific neoantigens, might be an appropriate approach.

The generation of such personalized immunotherapeutics requires time, as several steps like sequencing, data analysis, *in vitro* analysis, and agent production are very time consuming, which makes it inapplicable for some patients with end-stage

tumors. Due to the slow progression rate of most NETs, this problem might not apply for NET patients. We found that intra-tumoral heterogeneity is very limited in our case, which is also favorable for a personalized therapy.

As reconfirmed in this work, NETs acquire a relatively small number of mutations, in our case only 15 expressed non-synonymous somatic coding SNVs and four indels were detected.⁶ Epitope prediction on peptides containing these SNVs and on neoORF peptides generated by frameshift indels, revealed 28 epitopes that bind with high to intermediate affinity to one of the patient's HLA allele. We then synthesized these predicted neoantigens together with the corresponding wild-type peptides and conducted IFN γ ELISpot assays using the patient's peripheral blood to assess if there are T cells that are reactive against them. Our results showed pre-existing T cell responses against some of the tested peptides. Interestingly, most of the peptides with predicted high binding affinities did not show T cell reactivity in our ELISpot analysis. Only the RABEP1 mt and wt peptides which are considered strong



binders with a binding affinity of < 50 nM elicited a T cell response in the ELISpot. The wild-type peptide was predicted to bind slightly stronger, and this is also reflected in the ELISpot results, with the wild-type peptide having higher spot counts. MAT2A-mt3 is another epitope that showed T cell reactivity in the ELISpot. This neo-epitope was predicted to bind weakly with a binding score of 270 nM, whereas the wild-type counterpart MAT2A-wt3 was predicted to be a non-binder. The spot numbers in the ELISpot for MAT2A-wt3 were also not high enough to be considered significant; however, the difference to the spot counts of MAT2A-mt3 is not as obvious as the predicted binding affinities. Nevertheless, MAT2A-mt3 can be considered as a suitable neo-epitope for therapeutic vaccination. When looking at the neoORF epitopes generated through a frameshift-mutation in OBSL1, there are several neo-epitopes with high binding affinities. In the ELISpot however, only one neo-epitope, OBSL1-neoORF3 which has an intermediate predicted binding affinity of 188 nM, showed T cell reactivity. NeoORF epitopes are ideal candidates for therapeutic vaccination as there is no wild-type counterpart to those epitopes. In our case, the OBSL1 gene is additionally overexpressed in the tumor which makes the neo-epitopes harbored in this gene even better candidates.

Using the predicted neoantigens, synthetic vaccines may be produced and administered to the patient. Such therapeutic vaccines are supposed to aid in tumor control and several studies have shown the positive effects of neo-epitope vaccination. Yadav *et al.* for instance reported an increase of neo-epitope reactive CD8⁺ T cells upon a single immunization,³¹ and multiple studies have shown that CD8⁺ T cells that recognize neo-epitopes can attack tumors.^{30,36,37} ELISpot analysis for immunogenicity of the predicted neoantigens revealed three neo-epitopes with pre-existing T cell reactivity, MAT2A-mt3, RABEP1-mt, and OBSL1-neoORF3. Although, there seem to be no reactive T cells against the majority of the predicted neoantigens in the patient's peripheral blood, antitumor immunity could be induced through therapeutic vaccination. For a long time, it was controversially discussed among researchers, whether enhancement of an existing T cell response or generation of *de novo* responses is clinically relevant for an effective tumor vaccine.³⁵ Carreno *et al.* recently reported that neoepitope vaccination not only can amplify existing CD8⁺ T cell responses but also can produce responses that might have been silent prior to vaccination.³⁸ Thus, even if no T cell reactivity was seen for certain neoepitopes in the ELISpot assays, vaccination with them might still generate potent antitumor T cell responses.

If a therapeutic vaccine is going to be administered, immunization with multiple neoantigens is of advantage. In doing so, the likelihood of generating an immune response against at least some of the neoantigens increases, and the likelihood of the tumor escaping the immune response by immunoeediting decreases. Another option for the therapeutic usage of the patient-specific neoantigen repertoire is to create neoantigen-specific lymphocyte products *in vitro*, like for example, the adoptive transfer of *ex vivo*-activated autologous T cells and natural killer cells.

The immunohistochemical stainings for CD3, CD20, and NKp46 showed that the lymphocyte numbers at the metastatic

lesions are generally low. In line with this, staining for the modulatory molecules PD-1 and the corresponding ligand PD-L1 showed that these molecules are not prominent as well. Tumeh and colleagues have recently shown in melanoma patients, that the success of checkpoint blockade therapy against PD-1 depends on existing CD8⁺ T cells that are negatively regulated by PD-1/PD-L1.³⁹ Based on these findings, immune checkpoint therapy targeting PD-1 and its ligands seems not to be a suitable therapy option for our NET patient.

Compared to data from colorectal cancer liver metastases^{40,41} the cell densities of effector cells are dramatically low. In line with the clinical findings for low-proliferative NETs, this low infiltrating indicates a low chance of responding to chemotherapy. The ELISpot data suggest that there is pre-existing T cell reactivity against some neoantigens, showing interaction between tumor cells and the immune system, but apparently this interaction is not sufficient to allow higher infiltration of effector cells. An alternative explanation is the existence of other inhibitory signals that prevent effector T cell influx at the metastatic site.

The cytokine landscape of the metastatic sites shows a general absence of classical immunological effects within the microenvironment. Comparing the data to findings from metastatic colorectal cancer⁴² it is clear that there is not much immune activation present in this metastatic NET. MIF, VCAM-1, and ICAM-1 appear to be elevated due to the presence of tumor cells and are most likely observed in this context. It has been shown previously, that MIF expression is dramatically increased in hepatic metastases of colorectal cancer patients, and there are numerous studies suggesting a direct role of MIF in tumor pathogenesis and progression in different tumor entities.⁴³ Furthermore, anti-MIF therapeutics such as neutralizing anti-MIF antibodies have been shown to have a significant effect on tumor growth in colorectal cancer,⁴³ an option which might also apply to this case of metastatic NET.

Together, our results highlight the broad range and complexity of different levels of tumor–host immune interactions in a case of metastatic NET of the rectum. Using our integrative workflow, we have investigated various immunotherapeutic options and can suggest additional treatment approaches for this patient. Given the tremendous success of immunotherapy, such an integrative approach incorporating many aspects of the tumor–host immune setting, can be a valuable option for complex cases where no standard treatment is available.

Materials and methods

Patient sample

A 51-year-old Caucasian male was diagnosed with a rectal tumor in 2010. Pathology evaluation revealed a well-differentiated neuroendocrine tumor of the rectum. The patient underwent surgery in 2010, where the primary tumor and some liver metastases were resected, and subsequently most of the liver metastases were removed in 2012.

An OCT-embedded fresh-frozen sample from a liver metastasis resected in 2010 (LM1) was analyzed using WGS and RNA-Seq. Additionally, OCT-embedded fresh-frozen samples from five additional, distinct liver metastases resected in 2012

(LM2-LM6) were analyzed using WGS and RNA-Seq (Table 1). Whole-blood and healthy liver samples were used as germline control sequences.

Using the patient's blood, PCR-based HLA typing was performed in the HLA-Lab in the Institute for Immunology, University Hospital Heidelberg, Heidelberg, Germany. The patient's HLA genotype was shown to be: HLA-A*03:02, HLA-A*33:01, HLA-B*14:02, HLA-B*55:01, HLA-C*03:03, HLA-C*08:02.

The patient underwent leukapheresis and 10 mL of the leukapheresis product was used for ELISpot analysis.

The study was performed under an IRB approved protocol (AAAJ2008). The patient was consented under the same protocol.

Sequence data analysis

Sequence read pairs from WGS were mapped and aligned to the 1,000 genomes phase 2 reference genome hs37d5 as previously described,⁴⁴ using Burrows–Wheeler Aligner (BWA) (version 0.6.2), and were processed with SAMtools (version 0.1.17) and Picard tools (version 1.61).

Somatic single nucleotide variants (SNVs) were identified in the aligned sequences using an in-house analysis pipeline based on SAMtools mpileup and bcftools, as described previously.⁴⁴

Short insertions and deletions were called using an in-house pipeline based on platypus (0.5.2).⁴⁵ Since platypus was developed to detect variants in normal genomes, additional custom filters were added to reliably detect somatic indels in tumor normal pairs. These filters integrate the genotype likelihood as well as other filter criteria originally generated by platypus. All calls were annotated with annovar⁴⁶ using the gencode reference (v17). All somatic high-confidence indels that fall into a coding gene or a splice site were extracted and visually inspected.

RNA-Seq read pairs were mapped to the NCBI human reference genome build 37.2 using Tophat (version 2.0.4). All candidate DNA variant positions were annotated with RNA information as described previously.⁴⁷ Briefly, a candidate DNA variant was called expressed if one high-quality RNA read containing the same variant was present. RNA-Seq data was also used to assess gene expression levels in means of the reads per kilobase per million reads (RPKM) measure.

Epitope prediction

We used computational methods to predict the immunogenicity of non-synonymous tumor-specific mutations which were detected in the sequencing data. More precisely, HLA class I binding prediction was performed on amino acid peptides containing the non-synonymous mutations, and on peptides containing the corresponding reference residue. As T-cell recognition of peptides is crucially dependent on the ability of the HLA molecule to effectively bind the peptide, comparison of predicted binding affinities of the mutated and reference peptides can be used to assess the immunogenicity of the mutation and to detect neo-epitopes.

For peptide-HLA binding affinity prediction, we chose the NetMHCcons method which was developed at the Technical University of Denmark.⁴⁸ NetMHCcons is a consensus method

for MHC class I predictions, integrating the three state-of-the-art methods NetMHC, NetMHCpan, and PickPocket.^{49–51} Depending on how much training data is available for the HLA allele of interest, one of the three methods or a combination of them is used to give the most accurate prediction.

For each non-synonymous mutation, peptides of length 8–11 that contain the mutated residue were extracted from the corresponding protein sequence, and stored in Fasta files to be used as input files for the prediction algorithm. All possible combinations of peptide length and mutation position were considered. Analogously, Fasta files containing the reference peptides were generated. Novel tumor-specific peptides which were generated by frameshift insertions or deletions were also analyzed with NetMHCcons. These so called neoORF antigens are supposed to be highly immunogenic, as they provide longer, completely novel stretches of tumor-specific antigens.

Both, the mutated and reference sequences were submitted to the NetMHCcons 1.0 Server for each HLA allele of the patient, in order to perform allele-specific HLA class I binding predictions. The results of the prediction are IC50 values given in nanomolar (nM) affinity values. Peptides with less than 50 nM are considered as strong-binding, and those with less than 500 nM as weak-binding. Peptides with more than 500 nM are considered as non-binders.

ELISPOT

Cell preparation

Ten mL of leukapheresis product was freshly used for the analysis. Ficoll density gradient centrifugation was performed using 50 mL Leucosep tubes (Greiner Bio-One, Kremsmünster, Austria) to isolate PBMC. The median PBMC obtained was 1×10^8 . Thereof, T cells and dendritic cells (DCs) were purified as described previously.^{52,53} Briefly, T cells were cultured for 7 d in X-VIVO 20 medium containing 100 U/mL human rIL-2 (Proleukin, Chiron, Ratingen, Germany), and 60 U/mL human rIL-4 (Promokine, PromoCell, Heidelberg). Afterward, cells were kept in cytokine-free medium for 12 h and human CD3 T cells were purified using the Dynabeads untouched human T cell kit (Invitrogen, Darmstadt, Germany).

For DC maturation, adherent cells were cultured for 7 d in X-VIVO 20 medium containing 560 U/mL human rGM-CSF (Leukine, Berlex, Bayer, Leverkusen, Germany), and 500 U/mL human rIL-4. DCs were enriched using anti-CD56 coupled magnetic beads (C218, Beckman Coulter, Krefeld, Germany), and anti-CD3- and anti-CD19-Dynabeads (Invitrogen, Darmstadt, Germany), and pulsed for 18 h with $0.8 \mu\text{g}/\mu\text{L}$ test peptides or IgG. As positive control, $0.1 \mu\text{g}/\mu\text{L}$ staphylococcal enterotoxin B (SEB) was used.

Peptides

Peptides were produced by the Peptide Synthesis Facility of the DKFZ. Lyophilized synthetic peptides were solved in distilled water containing 10% DMSO. Peptide purity was >98%. Peptides were designed to contain the identified immunogenic HLA-restricted T cell epitope. Synthesized human IgG peptides as well as IgG (Kiovig, Baxalta, Unterschleißheim, Germany) were used as negative control antigens.

IFN γ ELISpot assay

ELISpot assays were done as described previously^{52,53} with modifications. The assay was carried out in X-VIVO 20 medium, which has been pretested for ELISpot performance in comparative testing with other media. On day 1, ELISpot plates (MAHA S45, Millipore, Eschborn, Germany) were washed with PBS and coated with 1 μ L per well of anti-IFN γ antibody. The plate was stored overnight at 4°C.

Peptide-pulsed DCs (2×10^4) were incubated with autologous T cells (1×10^5) at a 1:5 ratio for 40 h in ELISpot plates. All tests were performed in triplicate wells. Internal established operating procedures of an exploratory research laboratory were used for ELISpot testing.

IFN γ spots were measured using the automated system CTL ImmunoSpot analyzer (CTLEurope, Bonn, Germany). Each well was subjected to a manual quality control and was reviewed by an independent scientist. Counting parameters were established using the IgG control wells obtaining a high signal-to-noise ratio. Spots induced by the control peptide (human IgG) were considered as background reactivity. A reaction against a test peptide was considered a positive response according to predefined criteria if the spot counts were significantly ($p < 0.05$) higher than the IgG counts according to a permutation test using the difference in means as the test statistic. Raw data is accessible upon request.

Immunohistochemistry and cytokine detection

FFPE blocks of samples LM3, LM4, and LM5 were immunohistochemically analyzed for their infiltration with T cells (CD3e), B cells (CD20), and NK cells (NKP46), and for the expression of HLA and the immunomodulatory proteins PD-1 and PD-L1. The complete staining procedure was carried out on a BOND Max (Leica) and evaluated as previously described.^{42,54}

Tissue lysates were prepared from frozen material according to the manufacturer's instructions (Bio-Rad) and were used for cytokine detection, as previously described.^{42,54}

Disclosure of potential conflicts of interest

No potential conflicts of interest were disclosed.

References

1. Dong M, Phan AT, Yao JC. New strategies for advanced neuroendocrine tumors in the era of targeted therapy. *Clin Cancer Res* 2012; 18:1830-6; PMID:22338018; <http://dx.doi.org/10.1158/1078-0432.CCR-11-2105>
2. Bernick PE, Klimstra DS, Shia J, Minsky B, Saltz L, Shi W, Thaler H, Guillem J, Paty P, Cohen AM et al. Neuroendocrine carcinomas of the colon and rectum. *Dis Colon Rectum* 2004; 47:163-9; PMID:15043285; <http://dx.doi.org/10.1007/s10350-003-0038-1>
3. Moore JR, Greenwell B, Nuckolls K, Schammel D, Schisler N, Schammel C, Culumovic P, McKinley BP, Trocha SD. Neuroendocrine tumors of the rectum: a 10-year review of management. *Am Surg* 2011; 77:198-200; PMID:21337880.
4. Oberg K. The genetics of neuroendocrine tumors. *Semin Oncol* 2013; 40:37-44; PMID:23391111; <http://dx.doi.org/10.1053/j.seminoncol.2012.11.005>
5. Bergsland EK. Introduction: recent advances in the genetics, diagnosis, and treatment of neuroendocrine tumors. *Semin Oncol* 2013; 40:1-3; PMID:23391108; <http://dx.doi.org/10.1053/j.seminoncol.2012.12.001>
6. Crona J, Skogseid B. GEP- NETS UPDATE: Genetics of neuroendocrine tumors. *Eur J Endocrinol* 2016; 174:R275-90; PMID:27165966; <http://dx.doi.org/10.1530/EJE-15-0972>
7. Leotlela PD, Jauch A, Holtgreve-Grez H, Thakker RV. Genetics of neuroendocrine and carcinoid tumours. *Endocr Relat Cancer* 2003; 10:437-50; PMID:14713256; <http://dx.doi.org/10.1677/erc.0.0100437>
8. Bergsland EK. The evolving landscape of neuroendocrine tumors. *Semin Oncol* 2013; 40:4-22; PMID:23391109; <http://dx.doi.org/10.1053/j.seminoncol.2012.11.013>
9. Eggenberger JC. Carcinoid and other neuroendocrine tumors of the colon and rectum. *Clin Colon Rectal Surg* 2011; 24:129-34; PMID:22942794; <http://dx.doi.org/10.1055/s-0031-1285996>
10. Schumacher TN, Schreiber RD. Neoantigens in cancer immunotherapy. *Science* 2015; 348:69-74; PMID:25838375; <http://dx.doi.org/10.1126/science.aaa4971>
11. Sharma P, Allison JP. The future of immune checkpoint therapy. *Science* 2015; 348:56-61; PMID:25838373; <http://dx.doi.org/10.1126/science.aaa8172>
12. Aparicio S, Caldas C. The implications of clonal genome evolution for cancer medicine. *N Engl J Med* 2013; 368:842-51; PMID:23445095; <http://dx.doi.org/10.1056/NEJMra1204892>
13. Yap TA, Gerlinger M, Futreal PA, Swartz L, Swanton C. Intratumor heterogeneity: seeing the wood for the trees. *Sci Transl Med* 2012; 4:127ps10; PMID:22461637; <http://dx.doi.org/10.1126/scitranslmed.3003854>
14. Caldas C. Cancer sequencing unravels clonal evolution. *Nat Biotechnol* 2012; 30:408-10; PMID:22565966; <http://dx.doi.org/10.1038/nbt.2213>
15. Baldus SE, Schaefer KL, Engers R, Hartleb D, Stoecklein NH, Gabbert HE. Prevalence and heterogeneity of KRAS, BRAF, and PIK3CA mutations in primary colorectal adenocarcinomas and their corresponding metastases. *Clin Cancer Res* 2010; 16:790-9; PMID:20103678; <http://dx.doi.org/10.1158/1078-0432.CCR-09-2446>
16. Huyge V, Garcia C, Alexiou J, Ameye L, Vanderlinden B, Lemort M, Bergmann P, Awada A, Body JJ, Flamen P. Heterogeneity of metabolic response to systemic therapy in metastatic breast cancer patients. *Clin Oncol* 2010; 22:818-27; PMID:20554438; <http://dx.doi.org/10.1016/j.clon.2010.05.021>
17. Kidd EA, Grigsby PW. Intratumoral metabolic heterogeneity of cervical cancer. *Clin Cancer Res* 2008; 14:5236-41; PMID:18698042; <http://dx.doi.org/10.1158/1078-0432.CCR-07-5252>
18. Folprecht G, Gruenberger T, Bechstein WO, Raab HR, Lordick F, Hartmann JT, Lang H, Frilling A, Stoecklacher J, Weitz J et al. Tumour response and secondary resectability of colorectal liver metastases following neoadjuvant chemotherapy with cetuximab: the CELIM randomised phase 2 trial. *Lancet Oncol* 2010; 11:38-47; PMID:19942479; [http://dx.doi.org/10.1016/S1470-2045\(09\)70330-4](http://dx.doi.org/10.1016/S1470-2045(09)70330-4)
19. Whitelock JM, Melrose J, Iozzo RV. Diverse cell signaling events modulated by perlecan. *Biochemistry* 2008; 47:11174-83; PMID:18826258; <http://dx.doi.org/10.1021/bi8013938>
20. Euskirchen G, Auerbach RK, Snyder M. SWI/SNF chromatin-remodeling factors: multiscale analyses and diverse functions. *J Biol Chem* 2012; 287:30897-905; PMID:22952240; <http://dx.doi.org/10.1074/jbc.R111.309302>
21. Ye Y, Xiao Y, Wang W, Gao JX, Yearsley K, Yan Q, Barsky SH. Singular v dual inhibition of SNF2L and its isoform, SNF2LT, have similar effects on DNA damage but opposite effects on the DNA damage response, cancer cell growth arrest and apoptosis. *Oncotarget* 2012; 3:475-89; PMID:22577152; <http://dx.doi.org/10.18632/oncotarget.479>
22. Huang J, El-Gamil M, Dudley ME, Li YF, Rosenberg SA, Robbins PF. T cells associated with tumor regression recognize frameshifted products of the CDKN2A tumor suppressor gene locus and a mutated HLA class I gene product. *J Immunol* 2004; 172:6057-64; PMID:15128789; <http://dx.doi.org/10.4049/jimmunol.172.10.6057>
23. Linnebacher M, Gebert J, Rudy W, Woerner S, Yuan YP, Bork P, von Knebel Doeberitz M. Frameshift peptide-derived T-cell epitopes: a source of novel tumor-specific antigens. *Int J Cancer* 2001; 93:6-11; PMID:11391614; <http://dx.doi.org/10.1002/ijc.1298>

24. Saeterdal I, Bjrheim J, Lislrud K, Gjertsen MK, Bukholm IK, Olsen OC, Nesland JM, Eriksen JA, Moller M, Lindblom A et al. Frameshift-mutation-derived peptides as tumor-specific antigens in inherited and spontaneous colorectal cancer. *Proc Natl Acad Sci U S A* 2001; 98:13255-60; PMID:11687624; <http://dx.doi.org/10.1073/pnas.231326898>
25. Hacohen N, Fritsch EF, Carter TA, Lander ES, Wu CJ. Getting personal with neoantigen-based therapeutic cancer vaccines. *Cancer Immunol Res* 2013; 1:11-5; PMID:2477245; <http://dx.doi.org/10.1158/2326-6066.CIR-13-0022>
26. Heemskerck B, Kvistborg P, Schumacher TN. The cancer antigenome. *EMBO J* 2013; 32:194-203; PMID:23258224; <http://dx.doi.org/10.1038/emboj.2012.333>
27. Castle JC, Kreiter S, Diekmann J, Lower M, van de Roemer N, de Graaf J, Selmi A, Diken M, Boegel S, Paret C et al. Exploiting the mutanome for tumor vaccination. *Cancer Res* 2012; 72:1081-91; PMID:22237626; <http://dx.doi.org/10.1158/0008-5472.CAN-11-3722>
28. Matsushita H, Vesely MD, Koboldt DC, Rickert CG, Uppaluri R, Magrini VJ, Arthur CD, White JM, Chen YS, Shea LK et al. Cancer exome analysis reveals a T-cell-dependent mechanism of cancer immunoeediting. *Nature* 2012; 482:400-4; PMID:22318521; <http://dx.doi.org/10.1038/nature10755>
29. Duan F, Duitama J, Al Seesi S, Ayres CM, Corcelli SA, Pawashe AP, Blanchard T, McMahon D, Sidney J, Sette A et al. Genomic and bioinformatic profiling of mutational neopeptides reveals new rules to predict anticancer immunogenicity. *J Exp Med* 2014; 211:2231-48; PMID:25245761; <http://dx.doi.org/10.1084/jem.20141308>
30. Gubin MM, Zhang X, Schuster H, Caron E, Ward JP, Noguchi T, Ivanova Y, Hundal J, Arthur CD, Krebber WJ et al. Checkpoint blockade cancer immunotherapy targets tumour-specific mutant antigens. *Nature* 2014; 515:577-81; PMID:25428507; <http://dx.doi.org/10.1038/nature13988>
31. Yadav M, Jhunjunwala S, Phung QT, Lupardus P, Tanguay J, Bumbaca S, Franci C, Cheung TK, Fritsche J, Weinschenk T et al. Predicting immunogenic tumour mutations by combining mass spectrometry and exome sequencing. *Nature* 2014; 515:572-6; PMID:25428506; <http://dx.doi.org/10.1038/nature14001>
32. Robbins PF, Lu YC, El-Gamil M, Li YF, Gross C, Gartner J, Lin JC, Teer JK, Cliften P, Tycksen E et al. Mining exomic sequencing data to identify mutated antigens recognized by adoptively transferred tumor-reactive T cells. *Nat Med* 2013; 19:747-52; PMID:23644516; <http://dx.doi.org/10.1038/nm.3161>
33. van Rooij N, van Buuren MM, Philips D, Velds A, Toebes M, Heemskerck B, van Dijk LJ, Behjati S, Hilkmann H, El Atmioui D et al. Tumor exome analysis reveals neoantigen-specific T-cell reactivity in an ipilimumab-responsive melanoma. *J Clin Oncol* 2013; 31:e439-42; PMID:24043743; <http://dx.doi.org/10.1200/JCO.2012.47.7521>
34. van Buuren MM, Calis JJ, Schumacher TN. High sensitivity of cancer exome-based CD8 T cell neo-antigen identification. *Oncoimmunology* 2014; 3:e28836; PMID:25083320; <http://dx.doi.org/10.4161/onci.28836>
35. Fritsch EF, Rajasagi M, Ott PA, Brusica V, Hacohen N, Wu CJ. HLA-Binding Properties of Tumor Neopeptides in Humans. *Cancer Immunol Res* 2014; 2:1-8; PMID:24778159; <http://dx.doi.org/10.1158/2326-6066.CIR-13-0227>
36. Rooney MS, Shukla SA, Wu CJ, Getz G, Hacohen N. Molecular and genetic properties of tumors associated with local immune cytolytic activity. *Cell* 2015; 160:48-61; PMID:25594174; <http://dx.doi.org/10.1016/j.cell.2014.12.033>
37. Chan TA, Wolchok JD, Snyder A. Genetic Basis for Clinical Response to CTLA-4 Blockade in Melanoma. *N Engl J Med* 2015; 373:1984; PMID:26559592; <http://dx.doi.org/10.1056/NEJMc1508163>
38. Carreno BM, Magrini V, Becker-Hapak M, Kaabinejadian S, Hundal J, Petti AA, Ly A, Lie WR, Hildebrand WH, Mardis ER et al. Cancer immunotherapy. A dendritic cell vaccine increases the breadth and diversity of melanoma neoantigen-specific T cells. *Science* 2015; 348:803-8; PMID:25837513; <http://dx.doi.org/10.1126/science.aaa3828>
39. Tumeh PC, Harview CL, Yearley JH, Shintaku IP, Taylor EJ, Robert L, Chmielowski B, Spasic M, Henry G, Ciobanu V et al. PD-1 blockade induces responses by inhibiting adaptive immune resistance. *Nature* 2014; 515:568-71; PMID:25428505; <http://dx.doi.org/10.1038/nature13954>
40. Halama N, Michel S, Kloor M, Zoernig I, Benner A, Spille A, Pommerencke T, von Knebel DM, Folprecht G, Luber B et al. Localization and density of immune cells in the invasive margin of human colorectal cancer liver metastases are prognostic for response to chemotherapy. *Cancer Res* 2011; 71:5670-7; PMID:21846824; <http://dx.doi.org/10.1158/0008-5472.CAN-11-0268>
41. Halama N, Michel S, Kloor M, Zoernig I, Pommerencke T, von Knebel Doeberitz M, Schirmacher P, Weitz J, Grabe N, Jager D. The localization and density of immune cells in primary tumors of human metastatic colorectal cancer shows an association with response to chemotherapy. *Cancer Immunol* 2009; 9:1; PMID:19226101
42. Halama N, Braun M, Kahlert C, Spille A, Quack C, Rahbari N, Koch M, Weitz J, Kloor M, Zoernig I et al. Natural killer cells are scarce in colorectal carcinoma tissue despite high levels of chemokines and cytokines. *Clin Cancer Res* 2011; 17:678-89; PMID:21325295; <http://dx.doi.org/10.1158/1078-0432.CCR-10-2173>
43. He XX, Chen K, Yang J, Li XY, Gan HY, Liu CY, Coleman TR, Al-Abed Y. Macrophage migration inhibitory factor promotes colorectal cancer. *Mol Med* 2009; 15:1-10; PMID:19009023; <http://dx.doi.org/10.2119/molmed.2008.00107>
44. Jones DT, Hutter B, Jager N, Korshunov A, Kool M, Warnatz HJ, Zichner T, Lambert SR, Ryzhova M, Quang DA et al. Recurrent somatic alterations of FGFR1 and NTRK2 in pilocytic astrocytoma. *Nat Genet* 2013; 45:927-32; PMID:23817572; <http://dx.doi.org/10.1038/ng.2682>
45. Rimmer A, Phan H, Mathieson I, Iqbal Z, Twigg SR, Consortium WGS, Wilkie AO, McVean G, Lunter G. Integrating mapping-, assembly- and haplotype-based approaches for calling variants in clinical sequencing applications. *Nat Genet* 2014; 46:912-8; PMID:25017105; <http://dx.doi.org/10.1038/ng.3036>
46. Wang K, Li M, Hakonarson H. ANNOVAR: functional annotation of genetic variants from high-throughput sequencing data. *Nucleic Acids Res* 2010; 38:e164; PMID:20601685; <http://dx.doi.org/10.1093/nar/gkq603>
47. Jones DT, Jager N, Kool M, Zichner T, Hutter B, Sultan M, Cho YJ, Pugh TJ, Hovestadt V, Stutz AM et al. Dissecting the genomic complexity underlying medulloblastoma. *Nature* 2012; 488:100-5; PMID:22832583; <http://dx.doi.org/10.1038/nature11284>
48. Karosiene E, Lundegaard C, Lund O, Nielsen M. NetMHCcons: a consensus method for the major histocompatibility complex class I predictions. *Immunogenetics* 2012; 64:177-86; PMID:22009319; <http://dx.doi.org/10.1007/s00251-011-0579-8>
49. Lundegaard C, Lamberth K, Harndahl M, Buus S, Lund O, Nielsen M. NetMHC-3.0: accurate web accessible predictions of human, mouse and monkey MHC class I affinities for peptides of length 8–11. *Nucleic Acids Res* 2008; 36:W509-12; PMID:18463140; <http://dx.doi.org/10.1093/nar/gkn202>
50. Zhang H, Lund O, Nielsen M. The PickPocket method for predicting binding specificities for receptors based on receptor pocket similarities: application to MHC-peptide binding. *Bioinformatics* 2009; 25:1293-9; PMID:19297351; <http://dx.doi.org/10.1093/bioinformatics/btp137>
51. Zhang H, Lundegaard C, Nielsen M. Pan-specific MHC class I predictors: a benchmark of HLA class I pan-specific prediction methods. *Bioinformatics* 2009; 25:83-9; PMID:18996943; <http://dx.doi.org/10.1093/bioinformatics/btn579>
52. Bonertz A, Weitz J, Pietsch DH, Rahbari NN, Schlude C, Ge Y, Juenger S, Vlodavsky I, Khazaie K, Jaeger D et al. Antigen-specific Tregs control T cell responses against a limited repertoire of tumor antigens in patients with colorectal carcinoma. *J Clin Invest* 2009; 119:3311-21; PMID:19809157; <http://dx.doi.org/10.1172/JCI39608>
53. Horn T, Grab J, Schusdziarra J, Schmid S, Maurer T, Nawroth R, Wolf P, Pritsch M, Gschwend JE, Kubler HR et al. Antitumor T cell responses in bladder cancer are directed against a limited set of antigens and are modulated by regulatory T cells and routine treatment approaches. *Int J Cancer* 2013; 133:2145-56; PMID:23625723; <http://dx.doi.org/10.1002/ijc.28233>
54. Halama N, Zoernig I, Berthel A, Kahlert C, Klupp F, Suarez-Carmona M, Suetterlin T, Brand K, Krauss J, Lasitschka F et al. Tumoral Immune Cell Exploitation in Colorectal Cancer Metastases Can Be Targeted Effectively by Anti-CCR5 Therapy in Cancer Patients. *Cancer Cell* 2016; 29:587-601; PMID:27070705; <http://dx.doi.org/10.1016/j.ccell.2016.03.005>